

Solid Drops: Large Capillary Deformations of Immersed Elastic Rods

Serge Mora,^{1,*} Corrado Maurini,² Ty Phou,¹ Jean-Marc Fromental,¹ Basile Audoly,² and Yves Pomeau³

¹Laboratoire Charles Coulomb, UMR 5221, Université Montpellier 2 and CNRS, Place Eugène Bataillon, F-34095 Montpellier Cedex, France

²UPMC Université Paris 06 and CNRS, UMR 7190, Institut Jean le Rond d'Alembert, F-75005 Paris, France

³Department of Mathematics, University of Arizona, Tucson, Arizona 85721, USA

(Received 4 June 2013; published 10 September 2013)

Under the effect of surface tension, a blob of liquid adopts a spherical shape when immersed in another fluid. We demonstrate experimentally that soft, centimeter-size elastic solids can exhibit a similar behavior: when immersed into a liquid, a gel having a low elastic modulus undergoes large, reversible deformations. We analyze three fundamental types of deformations of a slender elastic solid driven by surface stress, depending on the shape of its cross section: a circular elastic cylinder shortens in the longitudinal direction and stretches transversally; the sharp edges of a square based prism get rounded off as its cross sections tend to become circular; and a slender, triangular based prism bends. These experimental results are compared to analysis and nonlinear simulations of neo-Hookean solids deformed by surface tension and are found to be in good agreement with each other.

DOI: [10.1103/PhysRevLett.111.114301](https://doi.org/10.1103/PhysRevLett.111.114301)

PACS numbers: 46.25.-y, 46.15.-x, 68.08.-p, 68.35.Gy

We all know that liquids can be shaped by surface tension: small droplets are spherical at equilibrium so as to minimize their area, and liquids climb on wet surfaces by making a smooth meniscus. The deformation of elastic solids by surface stress has been studied in more limited contexts. The macroscopic behavior of solids whose interfaces include features at the nanometer or micrometer scale, such as porous materials, has long been known to be influenced by the surface energy [1]. The smoothing effect of surface stress on finely textured solid interfaces has been pointed out [2,3]. The deformations of solids near a triple line (solid-liquid-vapor) have been understood recently [4–6]. Thin structures can be deformed by capillary forces very effectively, and many examples have been studied in the past few years [7–10].

In all these examples, the effect of surface stress is amplified by the roughness of the solid or by the presence of multiple interfaces—as happens near a triple line or when an elastic structure is partially covered by a liquid drop. Inspired by the canonical examples of spherical drops and bubbles, we ask the following question: can one change the shape of a smooth elastic solid just by immersing it into a fluid? We demonstrate that this is indeed possible using a centimeter-scale piece of elastic gel. Neither surface roughness nor a triple line is required: the solid is smooth and is immersed in a uniform fluid environment. As with drops and bubbles, the deformation is driven by the change in surface tension caused by immersion. Being both soft and slender, our gels are very flexible: their deformation can be measured by simple experimental techniques and quantitatively compared to model predictions.

To deform the gel, surface tension must work against the restoring elastic forces. This competition is ruled by the

elastocapillary length $\ell = \gamma/\mu$, where γ is the surface tension and μ the shear modulus. In usual solids, both γ and μ arise from phenomena at the atomic scale and ℓ is of the order of a nanometer. Our gels are extremely soft, having a shear modulus as low as $\mu = 35$ Pa; with $\gamma \sim 0.04$ N/m, the length scale $\ell \sim 1$ mm is large, making it possible to observe capillary effects in solids at the macroscopic scale [11–13]. The elastocapillary length ℓ is also relevant to instabilities deforming interfaces, such as the Biot [13,14], Rayleigh-Plateau [15], and Asaro-Tiller-Grinfeld instabilities [16].

In the experiments reported below, a prismatic mold made of polystyrene is first prepared by heating a preform supported by a rigid negative mold. A liquid is then introduced into the mold, which can be a hot aqueous solution of agar (from Alfa Aesar GmbH & Co) or a mixture of acrylamid and bisacrylamid (from Merck) in an aqueous solution. In both cases, a gel is formed after few hours at room temperature. The loss and storage moduli [17], measuring viscosity and elasticity, respectively, were measured in independent experiments done in similar conditions: after 3 h, the ratio of the loss modulus to the storage modulus is below 10^{-2} , indicating that the gel's response has become elastic. On the time scale of the experiment, we ignore the diffusion of the solvent inside the gel and towards the outer fluid: the gel is considered incompressible. Varying the nature of the gel and the concentration of its components, we can achieve shear moduli ranging from $\mu = 35$ to 350 Pa. Stress sweep tests reveal that the gel remains elastic well beyond a strain of 15% for agar and up to 500% for polyacrylamid gels, with a slight strain hardening above 150%.

A fluid interface is present along the boundary of the gel: the solvent, which remains trapped inside the gel, meets the

outer fluid along this boundary. This interface is associated with a surface energy (γA), where γ denotes the surface tension between the outer fluid and the solvent, and A is the area of the boundary. The surface energy drives the deformation of immersed gels, like that of drops and bubbles. It is resisted by the elasticity of the gel, which we model as an incompressible neo-Hookean material having a density of elastic energy $w = (\mu/2) \text{tr}(\mathbf{F}^T \cdot \mathbf{F} - \mathbf{1})$, where \mathbf{F} is the deformation gradient, $\mathbf{1}$ the unit matrix. The equilibrium is governed by the minimization of the free energy

$$\mathcal{E} = \gamma A + \iiint_{\Omega_0} \frac{\mu}{2} \text{tr}(\mathbf{F}^T \cdot \mathbf{F} - \mathbf{1}) dV_0, \quad (1)$$

where dV_0 is a volume element in reference configuration, Ω_0 is the reference volume occupied by the gel, and A is the area of the *deformed* boundary. The incompressibility constraint writes $J = \det \mathbf{F} = 1$.

In the general theory of surface stress in solids, the surface stress is anisotropic and is a function of the surface strain [18,19]. Our system is a special case: having a fluid origin, the capillary term in Eq. (1) corresponds to a surface stress that is both isotropic in the plane tangent to the boundary and independent of the strain. The surface tension γ between the outer fluid and the solvent can be measured independently; the comparison of experiments and models involves no adjustable parameter, even in the nonlinear regime.

We start with cross sections having the highest possible symmetry, namely, circular cylinders. Cylindrical molds with a radius ranging from $\rho_0 = 0.45$ to 2 mm and a length $L \approx 4$ cm are prepared, and an agar gel is formed inside the mold. Then, the polystyrene mold is immersed into liquid toluene and gets dissolved within few minutes; see the inset in Fig. 1. The gel is denser than toluene and sinks

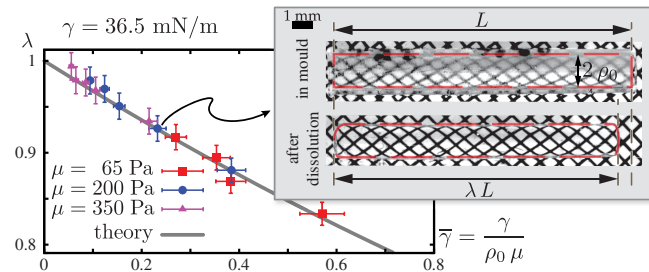


FIG. 1 (color online). Shortening of an initially circular cylinder made of agar gel when immersed in toluene. The axial stretch $\lambda \leq 1$ of a circular elastic cylinder is plotted for different values for the shear modulus μ and of the initial radius ρ_0 (in the range 0.45 to 2 mm), as a function of the dimensionless surface energy $\bar{\gamma}$. It is compared to the analytical formula in Eq. (2) (solid curve). Inset: Experimental pictures for $\mu = 200$ Pa and $\rho_0 = 0.8$ mm. The agar cylinder is formed inside a translucent mold (top); after dissolution of the mold, it lays on a hydrophobic grid and shortens as the result of surface stress (bottom). To aid visualization, the boundaries of the agar cylinder are highlighted using a dashed brown overlay.

until it reaches a horizontal grid placed at the bottom of the container. The grid is hydrophobic to prevent adhesion with the gel. The gel is imaged using a standard camera. It is always found to be shorter and thicker when immersed in toluene, compared to its initial shape set by the mold. Its surface appears to be smooth, consistent with the fact that the radius ρ_0 is larger than the critical radius of the Rayleigh-Taylor instability [15]. We measure the ratio $\lambda \leq 1$ of the final length to the initial length L , as a function of μ and ρ_0 . The values of λ collapse on a curve when plotted as a function of the dimensionless surface energy $\bar{\gamma} = \gamma/\rho_0\mu = \ell/\rho_0$ (Fig. 1). We use the independently measured water-toluene surface tension $\gamma = 36.5$ mN/m, as the gel's solvent is pure water. We have checked that the transverse expansion is consistent with our approximation of incompressibility. In view of the measured values of $\lambda \geq 0.85$, the agar gel remains below the elastic limit $(1 - \lambda) \sim 15\%$. The same phenomenon has been reproduced using polyacrylamid gels (data not shown).

The measurements of the stretch λ can be compared to a prediction based on Eq. (1). Assuming that the cylinder is long ($L \gg \rho_0$) and ignoring any end effect ($L \gg \gamma/\mu$), we seek a solution in the form of a homogeneous and biaxial deformation gradient \mathbf{F} . We use Cartesian coordinates (x, y, z) , the coordinate axis z being aligned with the cylinder's axis. Owing to the cylindrical symmetry and to the incompressibility, we write $\mathbf{F} = \lambda \mathbf{e}_z \otimes \mathbf{e}_z + \lambda^{-1/2}(\mathbf{e}_x \otimes \mathbf{e}_x + \mathbf{e}_y \otimes \mathbf{e}_y)$. The deformed lateral area is $A = (2\pi\rho_0/\lambda^{1/2})(\lambda L)$, where the first factor is the deformed perimeter proportional to the transverse contraction $\lambda^{-1/2}$, and the second is the length of the deformed cylinder proportional to the axial stretch λ . The area contributions coming from the disks at the ends are neglected. We insert these into Eq. (1) and use a thin disk $dV_0 = \pi\rho_0^2 dz_0$ as the undeformed volume element, with $0 \leq z_0 \leq L$. The resulting expression of the energy $\mathcal{E}(\lambda) = \frac{1}{2}\pi\rho_0^2 L \mu (4\bar{\gamma}\lambda^{1/2} + \lambda^2 + 2\lambda^{-1} - 1)$ is then minimized with respect to λ , which yields

$$\lambda = \left[\left(1 + \frac{\bar{\gamma}^2}{4} \right)^{1/2} - \frac{\bar{\gamma}}{2} \right]^{2/3}, \quad \text{where } \bar{\gamma} = \frac{\gamma}{\mu\rho_0}. \quad (2)$$

In Fig. 1, this prediction is shown to yield very good agreement with the experimental data with no adjustable parameter.

We now consider prismatic rods having an initially square cross section. After dissolution of the mold by toluene, the gel is transferred into silicon oil. Compared to toluene, silicone oils offers the advantage of having a much lower density mismatch $\Delta\rho$ with water: $\Delta\rho < 0.01$ g/cm³. This warrants that the ratio of the elastocapillary length ℓ to the gravity length $\mu/(g\Delta\rho)$ is smaller than 5×10^{-3} so that gravity can be neglected. We compared the deformed shapes of square based prisms having

the same dimensions and shear moduli: the agar gel was significantly more deformed than the polyacrylamid gel. This can be explained by the fact that the agar gel is deformed beyond its elastic limit (15%) in the neighborhood of sharp edges; there, the strain concentrates and has been argued to exceed 100% [2]. Therefore, we used polyacrylamid gels to study the deformation of sharp edges, as it has a very large elastic limit ($\sim 500\%$).

Experiments are carried out for different sizes of the initial cross section ($a_0 = 3$ to 6 mm) and for various values for the shear modulus ($\mu = 35, 60, 88,$ and 125 Pa). A longitudinal contraction was again observed. However, the most striking effect is that the initially square cross sections get rounded by surface tension; see Fig. 2(b). The rounding of an elastic wedge by surface tension has been simulated in earlier work [2], which focused on the neighborhood of the tip. The stress is large there, making the neo-Hookean law unreliable and the results of the simulation sensitive to the mesh (having tried to reproduce the simulation, we suspect that the finite tip curvature reported in Ref. [2] is due to the finite mesh size). This may explain why the quantitative predictions of this simulation have not been confirmed in experiments so far. We consider a *global measure* of the rounding of the cross sections instead, namely, the difference $\Delta\mathcal{A}$ between the area of the deformed cross sections and the area b^2 of the smallest square enclosing it, as sketched in Fig. 2(a). When the relative difference $\Delta\mathcal{A}/b^2$ is plotted as a function of the dimensionless surface stress $\bar{\gamma} = \gamma/a_0\mu = \ell/a_0$, as in Fig. 2(c), experimental points are found to collapse on a master curve. The rounding effect is more pronounced as

the ratio $\bar{\gamma} = \ell/a_0$ is smaller. Transferring the gel from oil into water, thereby suppressing the surface tension, we recover the original square cross sections: the deformation of the gel is elastic and reversible, and is driven by surface tension.

For square cross sections, the minimization of the energy (1) defines a nonlinear elasticity problem that has no analytical solutions. We carried out numerical simulations of a neo-Hookean solid deformed by surface tension, using the finite-element method (FEM) [20]. Assuming reflectional symmetry, we considered a domain of size $a_0/2 \times a_0/2 \times L/2$ and implemented the corresponding symmetric boundary conditions. An incompressible neo-Hookean model was used, including the effect of the surface energy. We adopted a set of units such that $a_0 = 1$ and $\mu = 1$ and varied the dimensionless surface tension $\bar{\gamma}$. The dimensionless measure of rounding $\Delta\mathcal{A}/b^2$ was implemented numerically as described earlier. The agreement between simulation [solid curve in Fig. 2(c)] and experiments is very good in the entire range of values of $\bar{\gamma}$ accessible in the experiments. Note that deformations are large: the rounding parameter $\Delta\mathcal{A}/b^2$ varies nonlinearly with surface tension, both in the simulation and in the experiments. A detailed comparison of the shapes of the lateral boundaries yields an excellent agreement, too [compare the solid red and dotted light blue curves in Fig. 2(b)]. To the best of our knowledge, these comparisons are the first quantitative test of the rounding of elastic solids by surface tension without any adjustable parameter.

We now consider the even less symmetric case of a prism whose base is an isosceles triangle: this leads to an entirely different type of deformation. We analyze the case of an infinitely long triangular prism subjected to small surface stress first: according to the theory of linear elasticity, the stress can be analyzed in the undeformed configuration. The surface tension is uniformly distributed along the triangular boundary; its component parallel to the axis of the prism is equivalent to a pointlike force applied at the centroid G of this boundary— G is called the *Spieker center* of the triangle; see Fig. 3(a). According to the theory of thin elastic rods, stretching and bending arise from the resultant force and moment of the applied load with respect to the centroid H of a cross section, respectively. In an isosceles but nonequilateral triangle, this point is distinct from the Spieker center G . As a result, the force equivalent to the surface tension, which is applied at G , induces both a compressive resultant force and a bending moment. The compressive force induces a contraction effect similar to that discussed earlier for circular cross sections. The bending effect is novel, however, and leads to large and easily measurable displacements. Calculating the position of the points G and H and using the linear beam theory, one finds the curvature κ of the centerline as a function of the height h of the cross section and of the apex angle θ as

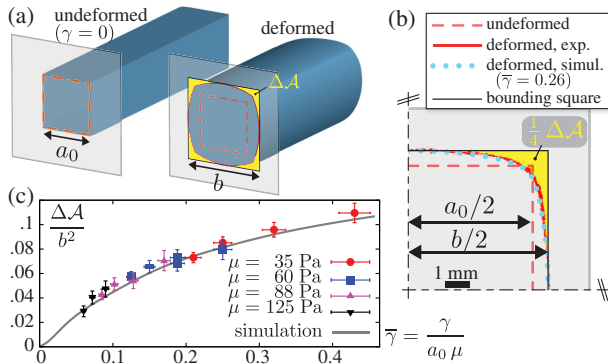


FIG. 2 (color online). Rounding of the edges of an initially square based prism made of polyacrylamid gel, immersed in silicone oil. (a) The amount of rounding is measured based on the surface area $\Delta\mathcal{A}$ defined in the text (yellow region). (b) Experimental shape of the cross section (solid red curve) for a shear modulus $\mu = 35$ Pa, surface stress $\gamma = 42.6$ mN/m, and initial edge length $a_0 = 5$ mm, and comparison to the simulation ($\bar{\gamma} = 0.26$, light blue dots). (c) The dimensionless measure of rounding $\Delta\mathcal{A}/a^2$ in the experiments is plotted as a function of the dimensionless surface stress $\bar{\gamma}$ for various initial cross-sectional widths a_0 and shear moduli μ , and compared to simulations (solid line).

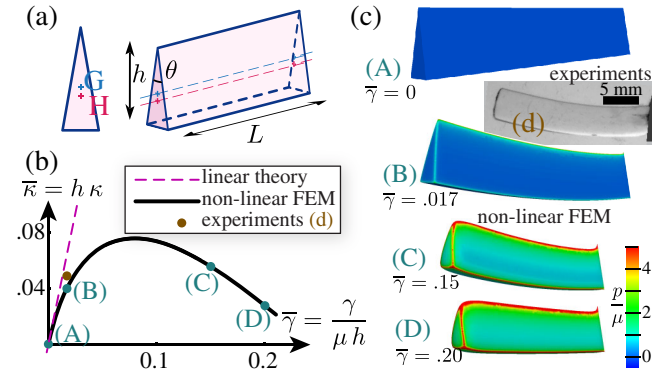


FIG. 3 (color online). Bending of a triangular prism by uniform surface stress. (a) Initial geometry. Note that the centroid H of the triangular cross section is distinct from the centroid G of its boundary, called the Spieker center. As a result, the uniform surface stress induces a nonzero bending moment. (b) Dimensionless curvature $\bar{\kappa}$ of a triangular prism with apex angle $\theta = 20^\circ$ and aspect ratio $L/h = 5.55$, as a function of the dimensionless surface stress $\bar{\gamma}$: nonlinear 3D finite element simulation for a neo-Hookean incompressible material and comparison to the linear beam theory from Eq. (3) for $L \gg h$ and $\bar{\gamma} \ll 1$. (c) 3D shapes of the deformed prism for selected values of $\bar{\gamma}$. The color code shows the pressure contribution p to the stress enforcing incompressibility. (d) Experimental evidence of bending of agar gels immersed in silicone oil ($h = 4.5$ mm, $L = 2.5$ cm, $\theta = 20^\circ$, $\bar{\gamma} = 0.0172$) and comparison to the corresponding finite-element simulation labeled (B).

$$\kappa = \frac{\bar{\gamma}}{h} \left(\frac{1}{\sin^2 \frac{\theta}{2}} - 2 \right), \quad \text{where } \bar{\gamma} = \frac{\gamma}{\mu h}. \quad (3)$$

By symmetry, this bending effect disappears in the equilateral case ($\kappa = 0$ when $\theta = \pi/3$), as well as for circular and square cross sections.

This bending effect has been confirmed in experiments using agar gel immersed in silicone oil; see the inset in Fig. 3(d). The choice of parameters is severely constrained by the applicability of the neo-Hookean model (requiring moderate strain), the accuracy in measuring curvature (requiring large surface tension and a good separation between the points H and G), and the need to keep the fabrication robust to imperfections: we used a length $L = 2.5$ cm, height $h = 4.5$ mm, and apex angle $\theta = 20^\circ$. The effect of surface tension is magnified by the slenderness of the rod and is visible to the naked eye: the measured radius of curvature is $r_{\text{exp}} = 9.5 \pm 1.5$ cm, corresponding to a dimensionless curvature $\bar{\kappa}_{\text{exp}} = h/r_{\text{exp}} = 0.049 \pm 0.008$. The experiment has been reproduced 3 times, yielding identical values of r_{exp} within 3%. Given the small surface energy $\bar{\gamma} = 0.0172$ ($\gamma = 42.6$ mN/m and $\mu = 550$ Pa), we would expect the linear theory (3) to be accurate, but it predicts a significantly larger curvature $\bar{\kappa}_{\text{lin}} = 0.065$. To explain this discrepancy, we set up FEM simulations that account both for the finite length and for nonlinear elasticity; see Fig. 3(c). The linear theory appears to be

accurate in a very narrow range $\bar{\gamma} = \ell/h \lesssim 0.005$. Beyond this, the cross sections become round and the curvature is overestimated. The nonlinear simulation predicts $\bar{\kappa}_{\text{simul}} = 0.040$ for $\bar{\gamma} = 0.0172$; see point (B) in Fig. 3(b), which matches the experimental value $\bar{\kappa}_{\text{exp}} = 0.049 \pm 0.008$ up to the experimental error bounds.

Although solids are often believed to deform in a fundamentally different way to fluids, we have shown that elastic rods made of soft gels can become rounded by surface tension when immersed into a liquid, much like bubbles. This rounding has been demonstrated at the centimeter scale and involves large, easily measurable deformation. Three specific modes of deformation have been identified—they can appear concurrently, as long as the symmetry of the cross sections allows it. A twisting mode is expected in the absence of a particular symmetry and could be investigated in future work. The phenomenon reported here gives a way to generate large, reversible deformations simply by changing the chemical properties of a liquid bathing a solid. This effect is stronger in filamentous structures which have a large area to volume ratio and are ubiquitous in biology. This opens up the possibility of tuning the texture of a hairy interface or actuating fibrous materials using surface tension.

*smora@univ-montp2.fr

- [1] H.L. Duan, J. Wang, Z.P. Huang, and B.L. Karihaloo, *J. Mech. Phys. Solids* **53**, 1574 (2005).
- [2] C. Y. Hui, A. Jagota, Y. Y. Lin, and E. J. Kramer, *Langmuir* **18**, 1394 (2002).
- [3] A. Jagota, D. Paretkar, and A. Ghatak, *Phys. Rev. E* **85**, 051602 (2012).
- [4] A. Marchand, S. Das, J.H. Snoeijer, and B. Andreotti, *Phys. Rev. Lett.* **108**, 094301 (2012).
- [5] R. W. Style, R. Boltyskiy, Y. Che, J. S. Wettlaufer, L. A. Wilen, and E. R. Dufresne, *Phys. Rev. Lett.* **110**, 066103 (2013).
- [6] R. Style and E. Dufresne, *Soft Matter* **8**, 7177 (2012).
- [7] C. Py, P. Reverdy, L. Doppler, J. Bico, B. Roman, and C.N. Baroud, *Phys. Rev. Lett.* **98**, 156103 (2007).
- [8] J. Hure, B. Roman, and J. Bico, *Phys. Rev. Lett.* **106**, 174301 (2011).
- [9] B. Roman and J. Bico, *J. Phys. Condens. Matter* **22**, 493101 (2010).
- [10] C. Duprat, S. Protière, and H. A. Stone, *Nature (London)* **482**, 510 (2012).
- [11] A. Lau, M. Portigliatti, E. Raphaël, and L. Léger, *Europhys. Lett.* **60**, 717 (2002).
- [12] A.R. Abate, L. Han, L. Jin, Z. Suo, and D. A. Weitz, *Soft Matter* **8**, 10032 (2012).
- [13] S. Mora, M. Abkarian, H. Tabuteau, and Y. Pomeau, *Soft Matter* **7**, 10612 (2011).
- [14] M. Ben Amar and P. Ciarletta, *J. Mech. Phys. Solids* **58**, 935 (2010).
- [15] S. Mora, T. Phou, J. Fromental, L. Pismen, and Y. Pomeau, *Phys. Rev. Lett.* **105**, 214301 (2010).

-
- [16] N. R. Bernardino and S. Dietrich, *Phys. Rev. E* **85**, 051603 (2012).
- [17] C. Macosko, *Rheology: Principles, Measurements and Applications* (Wiley-VCH, New York, 1994).
- [18] R. Shuttleworth, *Proc. Phys. Soc. London Sect. A* **63**, 444 (1950).
- [19] P. Muller and A. Saul, *Surf. Sci. Rep.* **54**, 157 (2004).
- [20] See Supplemental Material at <http://link.aps.org/supplemental/10.1103/PhysRevLett.111.114301> for the numerical method and a code to perform simulations.